To appear in:

Journal of Theoretical and Applied Physics

Online ISSN: 2251-7235 **Print ISSN: 2251-7227**

DOI: 10.57647/jtap.2026.8596.0306

Research Article

Creation of Avalanche Chain Reactions in $p^{11}B$ Fuel Using Magneto-Inertial Fusion

Fatemeh Namdari, Seyede Nasrin Hosseinimotlagh*

Department of Physics, Shi.C., Islamic Azad University, Shiraz, Iran

***Corresponding author:** nasrinhosseini _ motlagh@iau.ir, nasrinhosseinimotlagh@gmail.com

Received: 31 May 2025

Revised: 09 September 2025

Accepted:25 October 2026

ORCID: https://orcid.org/0000-0001-5381-2449

Abstract

A proton beam is produced at a velocity of the order of $10^9\ cm/s$ to interact with an uncharged hydrogen-boron medium such as H_3B. The generated charged particles are confined by electromagnetic fields. This is the basic concept of the new non-thermal fusion reactor. An external electric field is applied to prevent the energy loss of the proton particles by friction, due to their interaction with the electrons of the medium, to keep the proton-boron fusion at a maximum cross-section. Alphas produced by pB^{11} fusion undergo nuclear elastic collisions with surrounding protons, triggering a pB^{11} CR. The aim of this paper is to estimate the key parameters related to the performance of a new fusion reactor with neutron-free fusion fuel pB^{11} considering the production of alpha particle avalanches by presenting only the main physical processes and not a complete engineering design. To achieve this goal, a conceptual fusion reactor is proposed in this work using laser-plasma interactions and magnetic confinement configurations. The final result of our work considering this new reactor shows that it is possible to achieve fusion energy gain about 115, which is much higher than other cases examined.

Keywords: Magnetic confinement, Stopping power, CR, Electromagnetic fields, Laser, Fusion, Shock waves.

1. Introduction

Energy source of Sun and stars is nuclear fusion reactions. In the Sun, 4 protons combine and then an alpha particle is created. The confinement of hot solar plasma is carried out by the gravitational force resulting from the Sun's large mass. In Earth laboratories, the first reaction candidate for producing thermonuclear energy was DT reaction, which produced one neutron and an alpha with a released energy Q=17.6 MeV. The main reason for choosing DT is that the cross section of this reaction is the largest compared to other existing reactions. But one of the major problems with

the DT fuel is that it generates unwanted neutrons that can activate radioactive elements, and the availability of tritium in nature is very low, necessitating its artificial production.

One of the cleanest nuclear fusion reactions that avoids the problem of producing unwanted neutrons is the use of the neutron-free $p^{11}B$ fusion reaction, which ultimately produces three alpha particles. Using lasers, initially the number of 1000 reaction of $p^{11}B$ was measured just above the sensitivity level. Studies show that using high-energy proton beams produced by picosecond laser pulses and impinging them on an environment containing ^{11}B can drive more than a million $p^{11}B$ reactions.

Magneto-inertial fusion (MIF) is an approach to fusion that combines the compressional heating of inertial confinement fusion (ICF) with the magnetically reduced thermal transport and magnetically enhanced alpha heating of magnetic confinement fusion (MCF). From an MCF perspective, the higher density, shorter confinement times, and compressional heating as the dominant heating mechanism reduce the impact of instabilities. From an ICF perspective, the primary benefits are potentially orders of magnitude reduction in the difficult to achieve ρr parameter (areal density), and potentially significant reduction in velocity requirements and hydrodynamic instabilities for compression drivers. In fact, ignition becomes theoretically possible from $\rho r \leq 0.01$ g/cm^2 up to conventional ICF values of $\rho r \sim 1.0$ g/cm^2, and as in MCF, Br rather than ρr becomes the key figure-of-merit for ignition because of the enhanced alpha deposition [4]. Within the lower-ρr parameter space, MIF exploits lower required implosion velocities (2–100 km/s, compared to the ICF minimum of 350–400 km/s) allowing the use of much more efficient ($\eta \geq 0.3$) pulsed power drivers, while at the highest (i.e., ICF) end of the ρr range, both higher gain G at a given implosion velocity as well as lower implosion velocity and reduced hydrodynamic instabilities are theoretically possible. To avoid confusion, it must be emphasized that the well-known conventional ICF burn fraction formula does not apply for the lower-ρr "liner-driven" MIF schemes, since it is the much larger mass and ρr of the liner (and not that of the burning fuel) that determines the "dwell time" and fuel burn-up fraction. In all cases, MIF approaches seek to satisfy/exceed the inertial fusion energy (IFE) figure-of-merit $\eta G \sim 7$–10 required in an economical plant with reasonable recirculating power fraction. A great advantage of MIF is indeed its extremely wide parameter space which allows it greater versatility in overcoming difficulties in implementation or technology, as evidenced by the four diverse approaches and associated implosion velocities.

At the PALS facility in Prague, a few-hundred-Joule laser with a nanosecond pulse time interacts with fuel pellets including high concentrations of ^{11}B doped with crystals of Si, producing a million α particles. Also, at the ELI facility, about 10^{11} α particles are produced per each shot of laser. Two distinct warm fusion mechanisms such as MCF and ICF have been explored over the past 60 years.MCF uses high-intensity magnetic fields (several Teslas) and low-density plasma (10^{14} cm^3) to achieve temperatures of approximately 10 keV to drive fusion reactions. Whereas ICF is based on the fast heating and compression of target to very high densities [1] and temperatures, e.g. more than 5 keV for DT reactions.

To ignite target with low energy, it was suggested [1-3] to use propellants that separate the compression and combustion of the fuel. At the first the target is compressed, after that propellant ignites a low portion of the target while the α particles created heat the rest of fuel. This mechanism is known as FI (fast ignition). Since FI suffers from the problem that the laser pulse does not directly reach the compressed fuel [4], new designs have been proposed to utilize proton-boron fusion [5-6].The new scheme described can be used for compounds of proton-boron fusion [7] helium 3-deuterium ($D\ ^3He$), deuterium-lithium 6 ($D\ ^6Li$), and proton-lithium 6 ($p\ ^6Li$), proton-lithium 7 ($p\ ^7Li$) should be used. Among these reactions, in this paper, we propose that clean $p^{11}B$ fusion (without neutrons) produces 3 alpha particles:

$$p + {}^{11}B \rightarrow 3\ {}^{4}He + 9.9MeV \qquad (1)$$

This fusion novel method is presented in Figure 1.

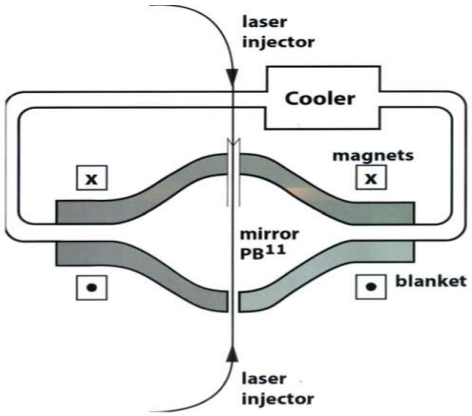

Figure 1. Schematic model of fusion reactor. Two ultra-intensities injected lasers, in the B-field mirror, initiate $p^{11}B$ nuclear fusion in the container. The generated α particles heat the fuel, which moves inside a cooler that recirculates the fluid of plasma with a density 1 mg/cm^3. Th deposited energy is carried out by the cooler, while the generated α particles are confined by external B-field.

2.Materials and methods

Lawson criterion in MCF

The ITER has been used successfully on the deuterium-tritium (D-T) fusion reactor, while the 14MeV-neutrons-induced damage and degradation would limit the useful lifetime of reactor component. The neutron production in p-^{11}B fuel is lower than that in D-T and deuterium-deuterium (D-D) fuel by orders of magnitude. Furthermore, hydrogen and boron are abundant and fairly accessible on earth, while ^{3}He might be mined and transported from the moon, which is one of the ingredients of deuterium-helium-3 (D-^{3}He) fuel. Therefore, there are sufficient reasons for us to pay more attention on proton-boron (p-^{11}B) fusion cycle. Since the core temperature of electrons is approaching the rest energy of electron, relativistic effect has to be considered in the extended tokamak system code to incorporate the relativistic bremsstrahlung. This extended tokamak system code is designed to include physics module, engineer module and economy module, the latter two of which are still under development and will be finished in the future work. Figure 2 illustrates that, Lawson criterion of D-T, D-^{3}He and D-D fusion reactor could meet at the same density of fuel ions, and the same ion and electron temperature whether in 0-dimensional model.

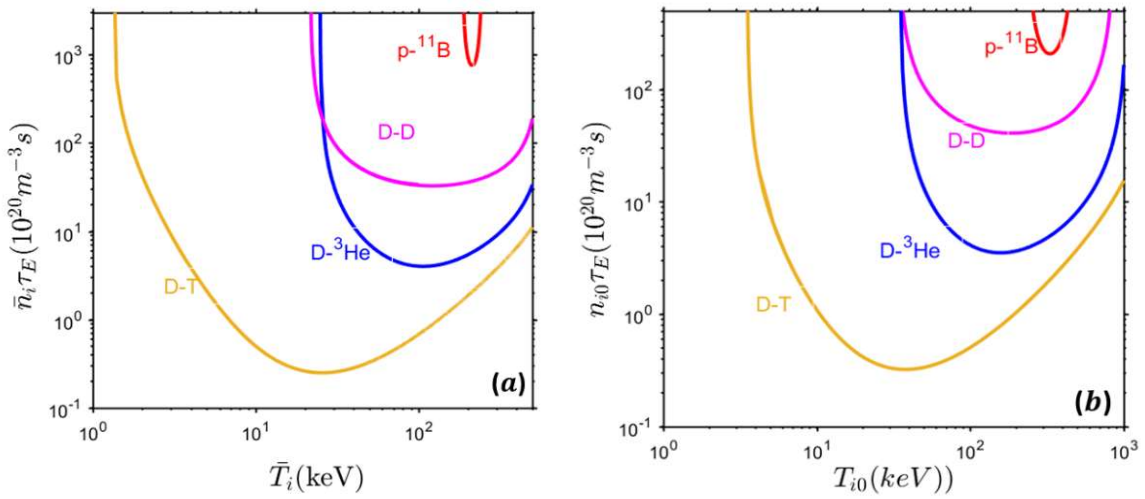

Figure2: $n_i\tau_E$ variations (a) in terms of volume averaged ion temperature $T_i$which meet Lawson criterion for D-T, D-^{3}He, D-D and p-^{11}B reactions with Q=1 in the 0-dimensional model.(b) in terms of core ion temperature T_{i0} which meet Lawson criterion for D-T, D-^{3}He, D-D and p-^{11}B reactions with Q=1 in the 1-dimensional model.[8]

Lawson criterion in ICF

A common metric for the performance of fusion power systems is the criterion first obtained by Lawson. In steady state, a plasma ignites if the ns product of number density and confinement time exceeds a specific value depending on the fusion reaction under consideration. The Lawson criterion is the statement of this minimum value, determined simply by $p_{fus} > p_{loss}$. Taking$p_{fus} = w_f n_a n_b < \sigma v >$, with w_f the energy released in charged particles, and defining $\tau = {}^{w}/_{(-\,dw/_{dt})}$, where w is the thermal energy content of the plasma and $-{}^{dw}/_{dt} = p_{brem} = p_{loss}$,$n_e\tau \geq \frac{T(z_b+z_a\epsilon)(1+z_b+\epsilon(1+z_a))}{w_f<\sigma\ >\epsilon}$, where $\epsilon = {}^{n_a}/_{n_b}$, $n_e = z_a n_a + z_b n_n$and T is the temperature common to all species. In general, the species temperatures differ, rendering the minimization of the right hand side nontrivial. It is however instructive to search numerically for those operating conditions which afford the least stringent Lawson criterion. The resulting numerical criterion is necessary but not sufficient for ignition. In pressure-limited systems, the triple product $nT\tau$ is a superior metric because it is proportional ${}^{T^2}/_{<\sigma v>}$, in turn inversely proportional to the achievable fusion power ${}^{w_f p^2 <\sigma v>}/_{T^2}$. Thus, the threshold igniting state has minimum $nT\tau$ and maximum power.

Minimum Lawson criterion for p-^{11}B shock wave ignition

The triple product criterion has the density scaling $min(nT\tau) \propto 8 + \frac{1}{\epsilon} + 15\epsilon$,which takes its minimum value at $\epsilon = {}^{n_a}/_{n_b} = {}^{1}/_{\sqrt{15}}$ Likewise, the quantity${}^{T^2}/_{<\sigma v>}$ is minimized for T =138 keV. This inconsistent optimization, regarding ϵ and T as totally independent quantities, returns an estimated lower bound of $5.1 \times 10^{23}\ {}^{keV.s}/_{m^3}$.However, a p-^{11}B plasma cannot ignite

with $T_e = T_i$. (That is, unless a very substantial number of x-rays can be reflected off the walls and reabsorbed by the plasma. Here, we assume that for all practical purposes, this cannot be done. We likewise assume that the plasma is optically thin to bremsstrahlung.) Per the analytic model, p_{fus}/p_{brem} *has a maximum value of 0.44 at* $T_e = T_i$=204keV and $\epsilon = 0.11$. A numerical search allowing for species-dependent temperatures found the extremal ignition point at a mass-weighted ion temperature T_{ion} =193 keV and $\epsilon = 0.26$. The corresponding minimum value of $nT\tau$ is $2.2 \times 10^{23}\ keV.s/_{m^3}$, in close agreement with the estimated value. The numerical optimum is cooler and significantly more boron-rich than the naiive minimization of $n_e\tau \geq \frac{T(z_b+z_a\epsilon)(1+z_b+\epsilon(1+z_a))}{w_f<\sigma v>\epsilon}$ would suggest. The extremal ignition state offsets a larger boron concentration (more fusions and bremsstrahlung) with a cooler T_e = 59 keV.

State-of-the-art of strong magnetic field generation

Conventional methods

State-of-the-art magnets nowadays allow generation of B-fields in the 10 − 300 T range, depending on their static/pulsed or destructive/non-destructive character [9]. Yet, conventional generation of strong magnetic field require special and very large magnet laboratory facilities.Following the studies initiated in 1920s by Kapitza and Wall [10] in magnet technology,33 T water-cooled magnets and a 45 T hybrid magnet have become available at the U.S National High Magnetic Field Laboratory (NHMFL) at Tallahasee and at the Nijmegen magnet laboratory now in operation in Netherlands. Several new laboratories with pulsed magnets have been established, and existing laboratories have been upgraded and modernized. The level of non-destructive "user" fields has been raised from 50 T to 70 T. In 2011, a record field close to 94.2 T has become available as the result of a European co-operative project at Dresden (HLD), adding a new dimension to pulsed field laboratories. This new dimension has been reached with the use of an incredible amount of 50 MJ (one of the world's largest capacitor bank) delivered over a pulse duration of ≈ 10 ms. However, fields at this record levels can only be obtained at the expense of a very short lifetime of the magnet, i.e. typically a few shots at the highest fields. The further development of the technology of non-destructive magnets is related to the development of more appropriate coil designs and the use of the strongest materials. Nevertheless, in spite of efforts of many laboratories, attempts to construct the magnets for multiple-use purposes with induction exceeding 100 T have failed. The maximum field that can be generated without destruction of the coil is determined by the mechanical strength of the coil, which must contain the Maxwell stress generated by the strong currents. This stress increases proportional to the square of the magnetic field ($B^2/2\mu_0$) and is approximately 4 GPa at 100 T, which is beyond the yield strength of the strongest materials now available such as maraging steel, electrically non-conducting fiber composites, or well-conducting macro- and micro-composite wires.

This reactor contains a background plasma with an order of density $^{mg}/_{cm^3}$ corresponding to hydrogen and boron ions. A solid fuel or plasma channel is irradiated by an ultra-intense laser, which produces a shock wave (SW) including hydrogen ions with energy range of 300-1200keV, which enters the background plasma. Alphas resulting from collide of boron with plasma protons and they accelerate and cause chain reactions (CRs). The number of α particles generated,N_α, which is written by the following equation:

$$N_\alpha \sim 3N_{\alpha 0}(e^{\tau/\tau_A} - 1) \quad (2)$$

Where $\tau_A \equiv \frac{1}{n_0<\sigma v>}$ such that $< \sigma v >$ which is known as fusion reactivity whose range of changes is 10^{-16} to $10^{-15}\frac{cm^3}{s}$. N_α is the number of α particles produced in CR time per the number of initial α particles $N_{\alpha 0}$. τ_A, is the CR time [8-9]. In the background plasma, the approximation value of n_0 is $10^{19}cm^{-3}$, and $< \sigma v > \sim 10^{-15}\frac{cm^3}{s}$, which corresponds to the time $\tau_A \sim 10^{-4}s$. During the interaction time of $\tau \sim 1ms$, Initially, we obtain an enhancement factor of 10^4 for the produced alphas. In this work, CRs and the confinement mechanism in novel reactor are presented. To continue the CR, this fusion reactor includes an external E-field and a system of magnetic confinement mirror for a long pulse to obtain an enhanced fusion energy gain. In Figure 3, we have drawn the diagram of $^{N_\alpha}/_{N_{\alpha 0}}$ variations in terms of $< \sigma v >$. As can be seen, the value of $^{N_\alpha}/_{N_{\alpha 0}}$ grows exponentially with the increase of $< \sigma v >$.

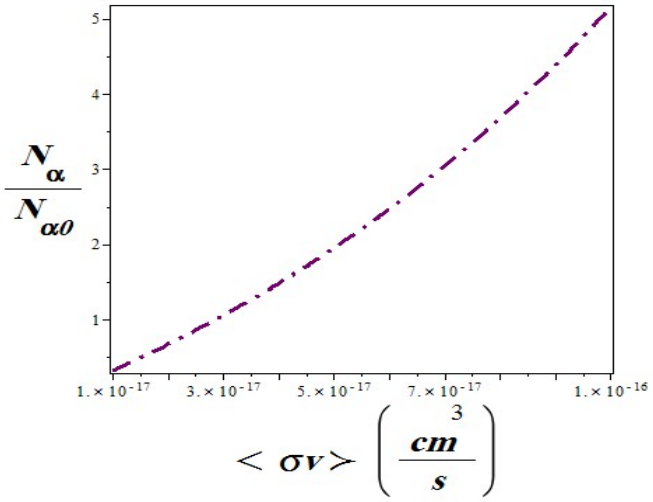

Figure 3. Variations of $^{N_\alpha}/_{N_{\alpha 0}}$ a function of $< \sigma v >$

3.The mechanism of SW triggering

In this device, two or even more SWs are generated via ultra-intense lasers. These SWs are semi-relativistic and travel at a SW speed of the order of 0.1c, where c is the velocity of light. The performance of these SWs has recently been reviewed in Ref. [11]. The SW generated by the laser is known as an accelerator that accelerates protons and borons in the SW domain with number densities n_p and n_B in volume. Here, we study two possibilities for creating a laser-generated shock wave: one for a gaseous fuel and the other for a solid fuel. In $p^{11}B$ center of mass frame the maximum fusion reactivity is:$< \sigma v > \sim 10^{-15}\, ^{cm^3}/_s$. There are two important points here: the first is that the laser is incident on a solid target consisting of boron and hydrogen in the inlet channel of Figure 1, and the second is that the laser generates a SW in the plasma gas [12]. SWs physics is wonderfully written in the book "Physics of SWs and high temperature hydrodynamic phenomena" [10]. An ultra-intense laser interaction with a planar fuel generates a 1-D SW [13]. The theory of laser-induced SWs, which has been investigated experimentally so far, is based on ablation of plasma.

For lasers with range of intensities $10^{12}\,{}^{W}/_{cm^2} < I_L < 10^{16}\,{}^{W}/_{cm^2}$ and nanosecond pulses, a hot plasma is generated. The hot plasma exerts a high pressure on the surrounding media, leading to the generation of a strong SW that travels inside the fuel. Here, quasi-relativistic SWs associated with the density of the solid or gas are of interest. The SWs induced by laser radiation in this region are studied via relativistic hydrodynamics [14]. Taub was the first to study relativistic SWs [15]. The SW equations of Figure 1 are written as follows:

$$(i)\ \frac{u_p}{c} = \sqrt{\frac{(P_1-P_0)(e_1-e_0)}{(e_0+P_1)(e_1+P_0)}}$$

$$(ii)\ \frac{u_s}{c} = \sqrt{\frac{(P_1-P_0)(e_1+P_0)}{(e_1-e_0)(e_0+P_1)}}$$

$$(iii)\ \frac{(e_1+P_1)^2}{\rho_1^2} - \frac{(e_0+P_0)^2}{\rho_0^2} = (P_1-P_0)\left[\frac{(e_0+P_0)}{\rho_0^2} + \frac{(e_1+P_1)}{\rho_1^2}\right] \tag{3}$$

Accordingly, P, e, and ρ are the pressure, energy density, and mass density, respectively, indices 0 and 1 indicate the areas before and after the SW enters, u_s is SW speed, and u_p is the speed of particle current and c is light velocity. It is assumed that in the laboratory reference frame the fuel is initially at the rest. The state equation used to estimate the SW key parameters which is the same as the state equation of ideal gas:

$$e_j = \rho_j c^2 + \frac{P_j}{\Gamma-1}; j = 0,1 \tag{4}$$

here Γ is known as specific heat ratio. We must solve equations (3) and (4) along with Piston's equation as follows [16]:

$$P_1 = \frac{2L_L}{c}\left(\frac{1-\frac{u_p}{c}}{1+\frac{u_p}{c}}\right) \tag{5}$$

It is easy to apply the dimensionless variables of pressure and laser irradiance that come from solving the above equations:

$$\Pi_L \equiv \frac{I_L}{\rho_0 c^3} \quad ; \quad \Pi = \frac{P_1}{\rho_0 c^2} \equiv \frac{P}{\rho_0 c^2} \tag{6}$$

In the area of transition between non-relativistic and relativistic SWs, related to the parameters of the SW, the following answers are obtained:

$$\frac{u_p}{c} = \sqrt{\frac{\Pi(2+\Pi)}{(1+\Pi)(\Gamma+1+\Pi)}} \approx 2\frac{(\Pi_L)^{1/4}}{(\Gamma+1)^{3/4}}$$

$$\frac{u_s}{c} = \sqrt{\frac{\Pi\Gamma+1+\Pi)}{(1+\Pi)(\Gamma+2)}} \approx \sqrt{2}\frac{(\Pi_L)^{1/4}}{(\Gamma+1)^{1/4}}$$

$$\Pi = (2\Pi_L)\left(\frac{1-{}^{u_p}/_c}{1+{}^{u_p}/_c}\right) \approx 2\sqrt{\frac{\Pi_L}{\Gamma+1}} \qquad (7)$$

In Figure 4, we plotted the two and three-dimensional variations of Π, $\frac{u_p}{c}$ and $\frac{u_s}{c}$ versus the parameters Π_L, ρ_0 and I_L (note that the two-dimensional diagrams for $\rho_0 = 10^{-3}\,{}^{g}/_{cm^3}$ and the range $10^{-4} \leq \Pi_L \leq 1$ are drawn). While the three-dimensional diagrams are drawn in the ranges of $10^{-4} \leq \rho_0 \leq 10^{-3}$ and $10^{12} \leq I_L \leq 10^{22}$). As can be seen the two-dimensional diagrams drawn in these figures related to the quantities Π, $\frac{u_p}{c}$ and $\frac{u_s}{c}$ show a non-linear behavior with the increase of Π_L.

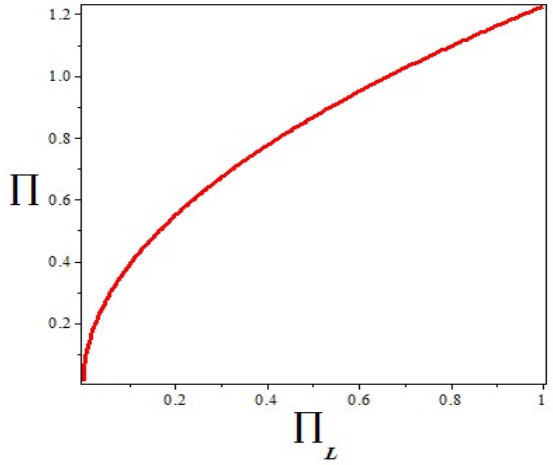

(a)

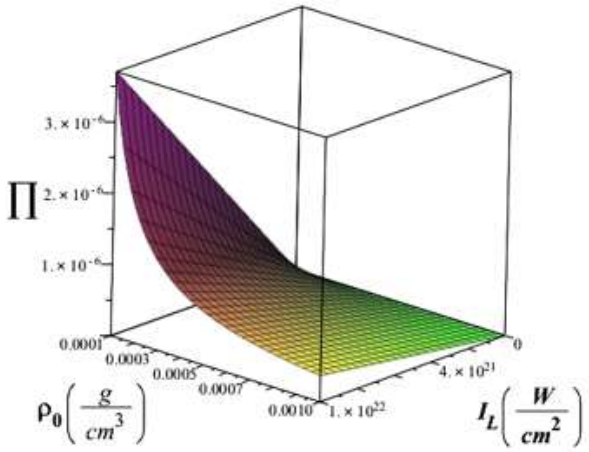

(b)

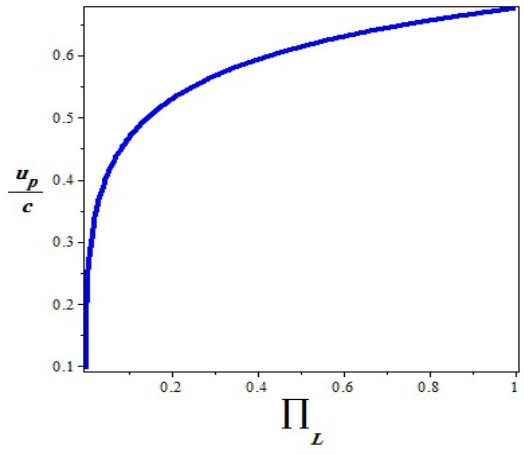

(c)

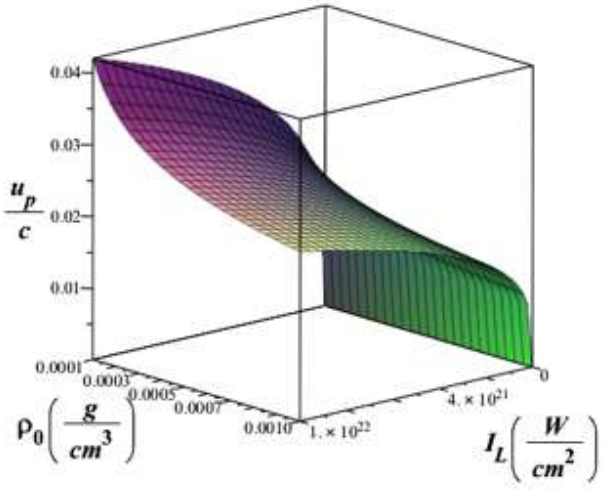

(d)

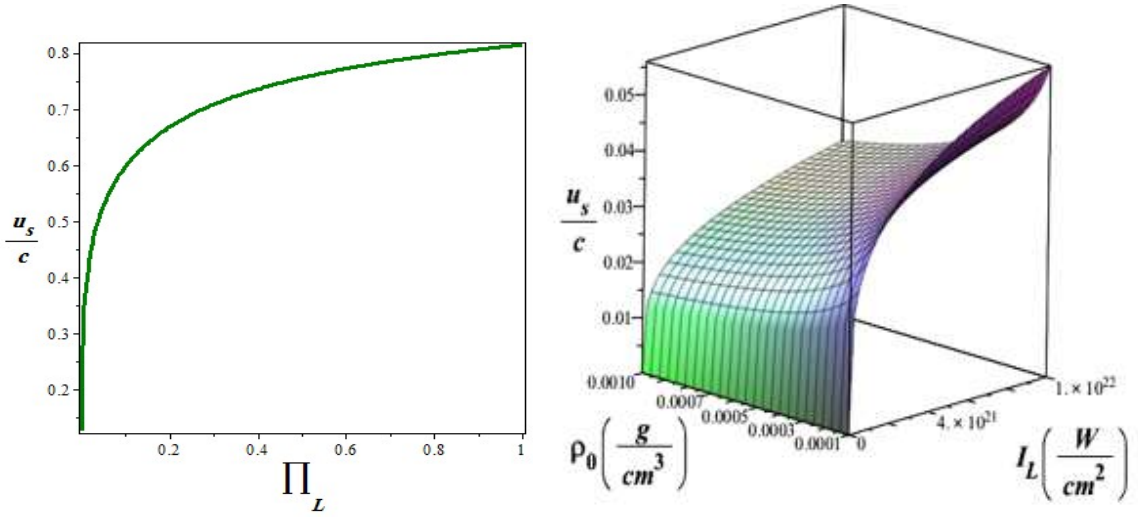

(e) (f)

Figure 4. 2 and 3D variations of ((a) and (b)) Π, ((c) and (d)) $\frac{u_p}{c}$ and ((e) and (f)) $\frac{u_s}{c}$ versus parameters Π_L, ρ_0 and I_L (note that the two-dimensional diagrams are drown for $\rho_0 = 10^{-3}\,{}^{g}/_{cm^3}$ and the range $10^{-4} \leq \Pi_L \leq 1$, while the three-dimensional diagrams are drawn in the ranges $10^{-4} \leq \rho_0 \leq 10^{-3}$)

Compression factor, $k = \frac{\rho}{\rho_0}$ depends on $\Pi = {}^{p}/_{\rho_0 c^2}$ and Γ. To view the transition between non-relativistic and relativistic approximation, relativistic equations must be solved to investigate the effects of the transition. Numerical calculations show an increase in the dimensionless SW velocity $\frac{u_s}{c}$ and particle velocity $\frac{u_p}{c}$ in the laboratory frame in terms of the dimensionless laser irradiation parameter $\Pi_L = {}^{I_L}/_{\rho_0 c^3}$. In addition, the speed of sound per speed of light, ${}^{c_s}/_{c}$, is given versus $\Pi_L = {}^{I_L}/_{\rho_0 c^3}$ and the diluted speed, c_{rw}, in the form of the following relationship:

$$\frac{c_s}{c} = \sqrt{(\frac{\partial P}{\partial e})_s} = (\frac{\Gamma P}{e+P})^{1/2} = [\frac{\Gamma(\Gamma-1)\Pi}{\Gamma\Pi + (\Gamma-1)k}]^{1/2}$$

$$c_{rw} = \frac{c_s + c_p}{1 + \frac{c_s c_p}{c^2}} \qquad (8)$$

In Figure 5, we have drawn the graphs of three-dimensional variations of $\frac{c_s}{c}$ and c_{rw} in terms of K and I_L parameters using the above equations.

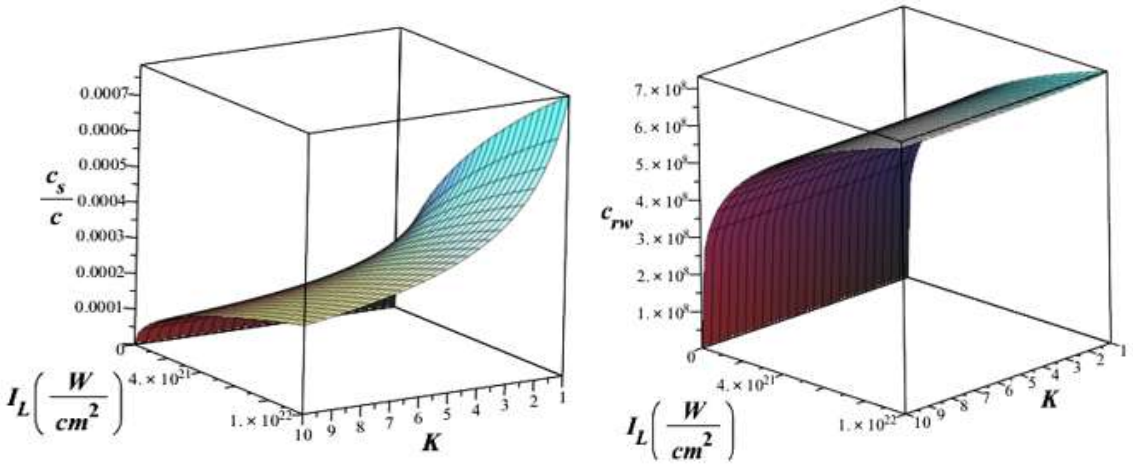

(a) (b)

Figure 5. The three-dimensional variations of (a) $\frac{c_s}{c}$ and (b) c_{rw} in terms of K and I_L parameters

The duration τ_{rw} in which the duration of the diluted wave reaching the front of shock, for the mode where the laser pulse duration in terms of τ_L, is given by:

$$\tau_{rw} = \frac{c_{rw}\tau_L}{c_{rw}-u_s} \qquad (9)$$

For a laser energy W_L and irradiation I_L and, we now calculate the duration of the laser pulse τ_L for the design under consideration to have a reasonable 1D SW I_L versus the velocity of flow u_p and the environment density is ρ_0, which means as follows:

$$I_L\left(W/_{cm^2}\right) = 2.2\times10^{18}\left(\frac{\rho_0}{10^{-3}g/_{cm^3}}\right); S(cm^2) = \pi R_L^2 = 4.5\times10^{-7}\left(\frac{10^{-3}g/_{cm^3}}{\rho_0}\right)\left(\frac{W_L}{1\,kJ}\right)\left(\frac{1ns}{\tau_L}\right);$$

$$R_L(\mu m) = 0.12\left[\left(\frac{10^{-3}g/_{cm^3}}{\rho_0}\right)\left(\frac{W_L}{1\,kJ}\right)\left(\frac{1ns}{\tau_L}\right)\right]^{0.5}; R_L(\mu m) \gg u_s\tau_L(\mu m) = 1.40\times 10^4\left(\mu m/_{ns}\right)\tau_L(ns) \qquad (10)$$

To solve equation (10), we replace the symbol ≫ is replaced by 5, that is, the diameter of laser is larger than a factor of 10 compared to the wavelength of shock during the time of laser pulse, $u_s\tau_L$, and we obtain:

$$\tau_L(ns) = 1.200\times10^{-3}\left(\frac{10^{-3}g/_{cm^3}}{\rho_0}\times\frac{W_L}{1\,kJ}\right)^{-3} \qquad (11)$$

That is, for the design where $I_L = 2.2\times10^{18}\,W/_{cm^2}$, if the energy of laser is 1 kJ, we required a pulse of laser equal to 1.2 ps. We plotted, the I_L variations in terms of ρ_0 with considering equation (10) in Figure 6. As can be seen from it, the value of I_L increases linearly with the increase of ρ_0.

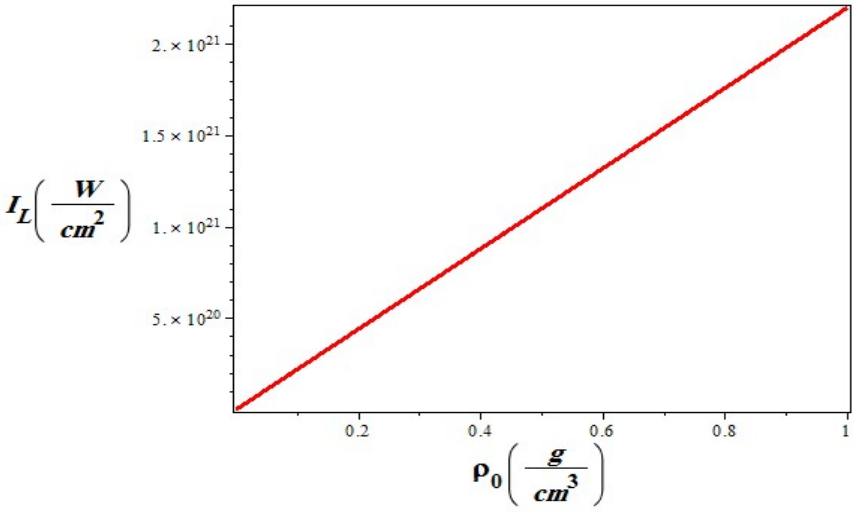

Figure 6. variations of I_L in terms of ρ_0 in the range of $10^{-4} \leq \rho_0 \leq 1$.

Also, using the relationships in equation (10), to estimate the numerical values of τ_L, S, and R parameters, three-dimensional variations of τ_L, S, and R in terms of ρ_0 and W_L have been drawn and shown in Figure 7.

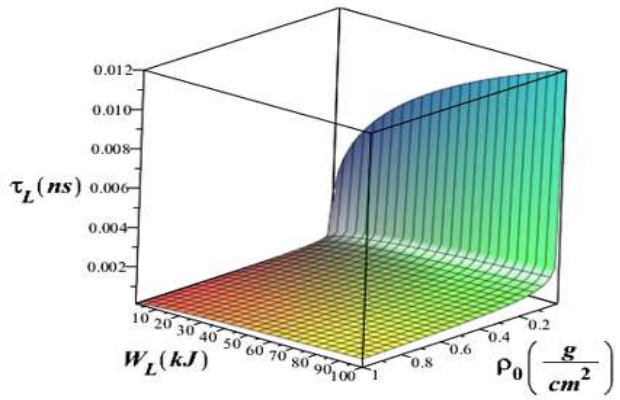

(a)

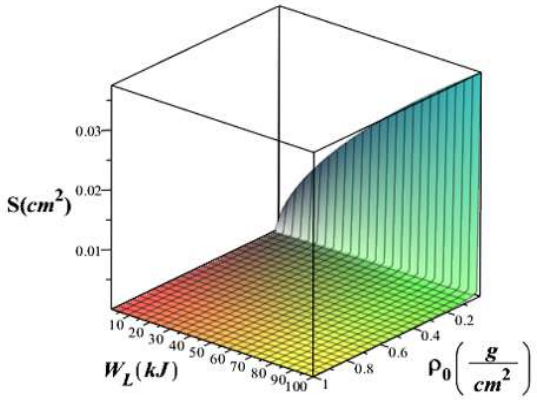

(b)

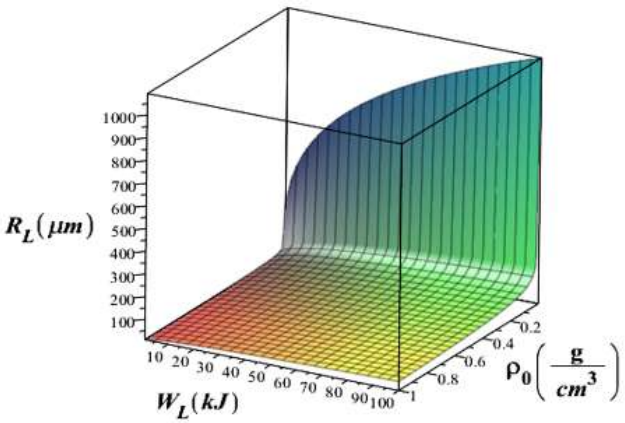

(c)

Figure 7. Three-dimensional variations of (a) τ_L,(b) S, and (c) R in terms of $\rho_0$and W_L in the range of $10^{-4} \leq \rho_0 \leq 1$ and $1 \leq W_L \leq 100$

4. Confinement mechanism of CRs

To prevent protons and α particles from going away from the walls of the container, we apply a magnetic mirror enclosure. For a longitudinal B-field in the container, the transverse radius of the target container is $2R_\alpha$, here R_α is the Larmor α radius, which is equal to:

$$R_\alpha = \frac{\gamma\beta_\perp M_\alpha c^2}{2e} \quad \beta_\perp = \frac{V_\perp}{c} \quad \beta = \frac{v}{c} \quad \gamma = \frac{1}{\sqrt{1-\beta^2}} \qquad (12)$$

M_α is the rest mass of the alpha particle which is about four times the mass of the proton and its kinetic energy is about 2.9 MeV, e is equal to $1.6 \times 10^{-19}C$, B is the longitudinal B-field, and $V_\perp$ is the velocity perpendicular to the B-field. For $\beta = 0.00387$ we have: $\gamma - 1 = 0.000075$ and for a B=25 Tesla, R_α is approximately 1 cm. This volume is controlled by it $B_{max}$and B_{min}, therefore the mirror ratio $R_m$is given by:

$$R_m = \frac{B_{max}}{B_{min}} \qquad (13)$$

The minimum value of the container V_v per $R_m = 1.5$ is: $V_v = \pi R^2 L = 16\pi R_\alpha^3$; $R = 2R_\alpha$; $L = 4R_\alpha$. Therefore, the alphas mirror confinement requires a V_v~$50cm^3$. It should be noted that the volume can be increased in a way that can maintain an appropriate fusion energy so that the container temperature does not exceed several eV [8]. In this design, we use a CR that is defined as an avalanche process. The mechanism of the CR through elastic collisions is described in the following:

(1) The 1st collision occurs between an α particle produced by the $p^{11}B$ fusion reaction (E_α energy) and a hydrogen ion in the desired container. (2) in the 2nd step, this alpha particle collides with another hydrogen ion in the container, such that (3) collides with a ^{11}B inside the container to fuse and generation of 3 α particles. So, the α particle with E_α energy performs its 2nd collision with a hydrogen ion and this hydrogen ion collides with a ^{11}B in the CM reference frame, the energy of CM,$E_{cm}(p^{11}B)$, gives the result:

$$E_{cm}(p^{11}B) = (\tfrac{11}{12})(\tfrac{16}{25})(\tfrac{9}{25})E_\alpha \cong 0.21E_\alpha \qquad (14)$$

Energy generated by the fusion reaction of $p^{11}B$ is divided equally between the 3 α particles, so $E_{cm}(p^{11}B)$ becomes ~600keV. New experimental data related to $p^{11}B$ have provided a σ_{max} for an α particle with 6 MeV energy, and the rest energy (2.9 MeV) being statistically divided between the other 2α particles.

The alphas spectrum generated in $p^{11}B$ reaction does not vary the concept of the reactor. To estimate this spectrum effect on the number of α particles generated (N_α) in the during of CR per initial number of α particles ($N_{\alpha 0}$) by the laser produced SW, having a numerical value of $<\sigma v>$ becomes necessary [17-18]. Here we present how to maintain CR for a long time, which is greater than the pulse duration. This is achieved with an external B-field and an E-field for acceleration, which acts like a cyclotron for p and α. These electromagnetic fields delay the alpha

particle avalanche production mechanism by overcoming the Beth Bloch energy dissipation in the external B-field. The stopping power of Bethe-Bloch, dT / dx, is written by:

$$\frac{dT_A}{dx}\left({}^{erg}/_{cm}\right) = -\frac{4\pi Z_A^2 Z_B e^4 n_0}{m_e c^2 \beta^2}\left[\ln\left(\frac{2m_e c^2 \beta^2 \gamma^2}{I}\right) - \beta^2\right]$$

$$\beta = \frac{u}{c}\ ;\gamma = \frac{1}{\sqrt{1-\beta^2}} = 1 + \frac{T_A}{M_A c^2} \qquad (15)$$

and in the non-relativistic state we have: $T_A = \frac{1}{2} M_A c^2 \beta^2$. The projectile (for example, proton here) with charge $Z_A e$ and mass M_A losses its energy through interaction with the surrounding electrons in the environment (for example, H_3B). T_A is the A projectile kinetic energy, βc is projectile velocity, index B indicates the environment. The environment density is n_0 , m_e is the electron mass, and $I(\sim 10\ \text{eV})$ is a constant that describes the electrons dependency on the environment. In the following the stopping power is given [19]:

$$\frac{dT_A}{dx}\left({}^{eV}/_{cm}\right) = -1.65 \times 10^7 Z_A^2 Z_B \left(\frac{n_0}{10^{22} cm^{-3}}\right)\left(\frac{0.04}{\beta}\right)^2 \qquad (16)$$

The intensity of the E-field is proportional to $(dTA/dx)/(Z_A e)$ .For our case $Z_A = 1$ (proton), $Z_B = 2$ (H_3B), $\beta = 0.035$ and for practical purposes it is conceivable to take $n_0 = 10^{19}$ [cm^{-3}], yielding an electric field of E=43 kV/cm. In Figure 8, we have drawn two and three-dimensional variations of $\frac{dT_A}{dx}$ in terms of β and n_0 according to equation (16). It should be noted that the two-dimensional graph is drawn for $\beta = 0.035$.

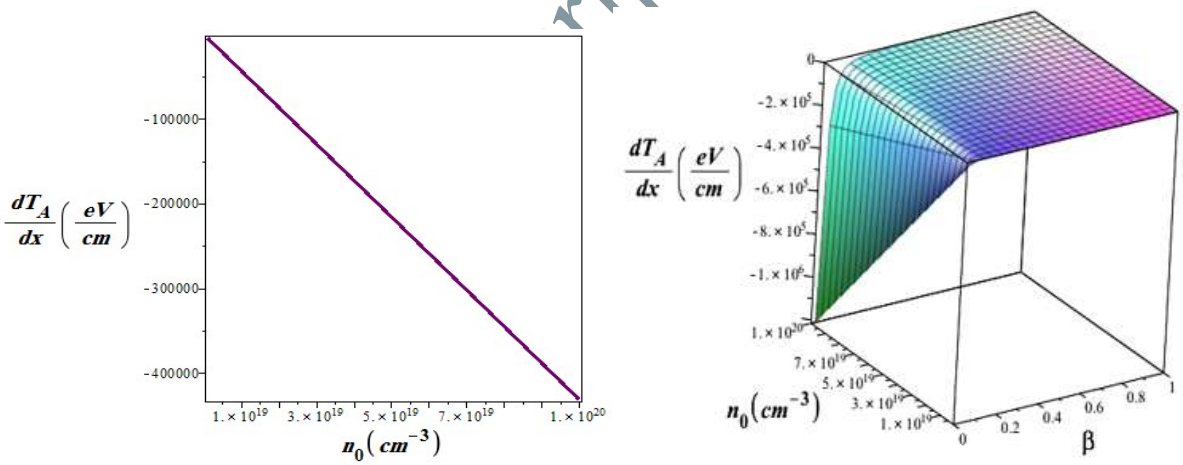

(a) **(b)**

Figure 8. (a) Two and (b) three-dimensional variations of $\frac{dT_A}{dx}$ in terms of β in the range of $0 \le \beta \le 1$ and $10^{18} \le n_0 \le 10^{20}$ (note that the two-dimensional diagram is related to $\beta = 0.035$)

A pulsed and oscillating field is preferred because higher peak values can be achieved here than a static field. In particular, one can use the oscillating electric field with respect to B-field at the ω_c written by the following equation:

$$\omega_c = \frac{Z_A e B}{M_A c}(Gaussian\ cgs\ units); M_A = AM_p$$

$$\omega_c\left(^{rad}/_{s}, proton\right) = 9.58 \times 10^8 [\frac{B}{10[Tesla]}] \qquad (17)$$

E_{ac} (Breakdown field) for the ac field is much larger than the dc mode and is roughly defined by the following relation [19-21]:

$$E_{ac} \approx \frac{m_e \omega_c c}{e} \approx 43(^{kV}/_{cm})(\frac{B}{25Tesla}) \qquad (18)$$

The steps in the avalanche of the $p^{11}B$ reaction are: In the first step (i) an alpha particle produced by the fusion of $p^{11}B$collides with a proton (which is at rest in the laboratory frame of reference) and in the second step (ii) this alpha particle has a second collision with another proton in the environment (which is at rest). This energetic proton with energy $W_{p'}$interacts with a ^{11}B from the environment (which is at rest) (iii) and three new alpha particles are produced. So that: $(i)\ p + B^{11} \rightarrow \alpha_1 + \alpha_2 + \alpha_3$;$(ii)\alpha_1 + H(rest.lab) \rightarrow \alpha_1' + p' + e$; $(iii)p' + {}^{11}B(rest.lab) \rightarrow \alpha_1 + \alpha_2 + \alpha_3 + 11e$. The density of the number of alpha particles produced n_α in NF$p^{11}B$ is related to the number density of proton n_p:

$$n_p = n_{p0} + \delta n_p \qquad ; \quad \delta n_p = {}^{n_\alpha}/_{3} \qquad (19)$$

Numerical densities (cm^{-3}) related to boron11 (n_B), protons (n_p) are [19]:

$$\varepsilon = \frac{n_B}{n_P} \quad ; n_0 = n_B + n_p = (\varepsilon + 1)n_p$$

$$n_p = 5.0 \times 10^{19}\left(\frac{\rho}{10^{-3}\,{}^{g}/_{cm^3}}\right) for\ \varepsilon = {}^{1}/_{3}$$

$$n_B = 51.66 \times 10^{19}\left(\frac{\rho}{10^{-3}\,{}^{g}/_{cm^3}}\right) for\ \varepsilon = {}^{1}/_{3} \qquad (20)$$

We prevent the deceleration of protons by an external electric field in the H_3B environment given by Eq.18. [22] So that the CR gives the density of the number of produced alpha particles n_α:

$$\frac{dn_\alpha}{dt} = n_B < \sigma v > (3n_{p0} + n_\alpha)$$

$$n_\alpha = 3n_{p0}[exp(n_B < \sigma v > t - 1)] \cong 3n_{p0}[exp\left(\frac{t}{\tau_A}\right) - 1]$$

$$\tau_A = \frac{1}{n_B < \sigma v >} \approx 4.8 \times 10^{-5}\left(\frac{10^{-3}\,{}^{g}/_{cm^3}}{\rho}\right) for\ \varepsilon = {}^{1}/_{3} \qquad (21)$$

The rate of proton production from CRs is described by the following equation:

$$\frac{dn_p}{dt} = n_H n_\alpha \sigma_{el} v_\alpha - n_p n_B \sigma_{fus} v_p \qquad (22)$$

In the above equation n_p is the proton density created after an alpha collision and destroyed after fusion occurs, as described by (i) and (ii). σ_{el} and $\sigma_{fus}$are the elastic and fusion cross sections, respectively, and v_α is the proton-alpha relative velocity before the elastic collision, while v_p is

the boron-proton relative velocity in the fusion reaction. In principle, equation (22) should include the recombination terms, however, it is expected that under ambient conditions the recombination rate will be very small [23-24]. The total elastic cross section of the alpha proton, σ_{el} is given by: $\sigma_{el}(\alpha.\,p) \cong \pi\left(\frac{e^2}{\mu v_\alpha^2}\right)^2$ where $\mu = \frac{4}{5}\,m_p$ (The reduced mass of the alpha-proton is) and $v_\alpha$is Alpha-proton relative velocity such that: $\sigma_{el} \sim 10^{-24}cm^2$[22]. We are interested in the fusion rate $p^{11}B$, i.e., $\sigma_{fus}v_p$, where σ_{fus} is the fusion cross-section, determined experimentally, and $v_p$is the relative velocity of $p^{11}B$.

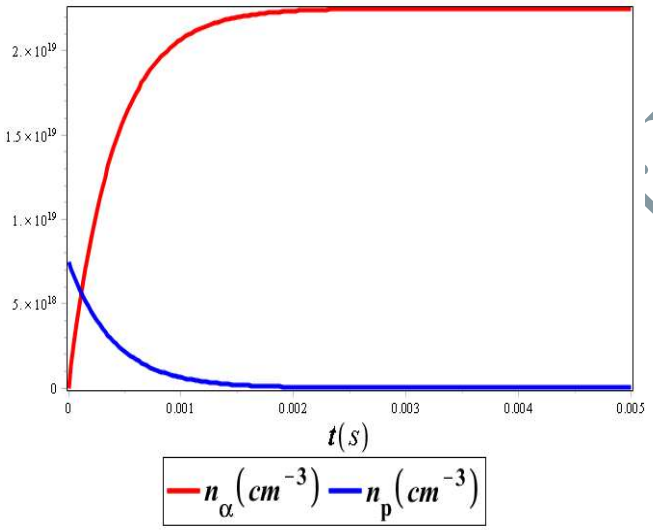

(a)

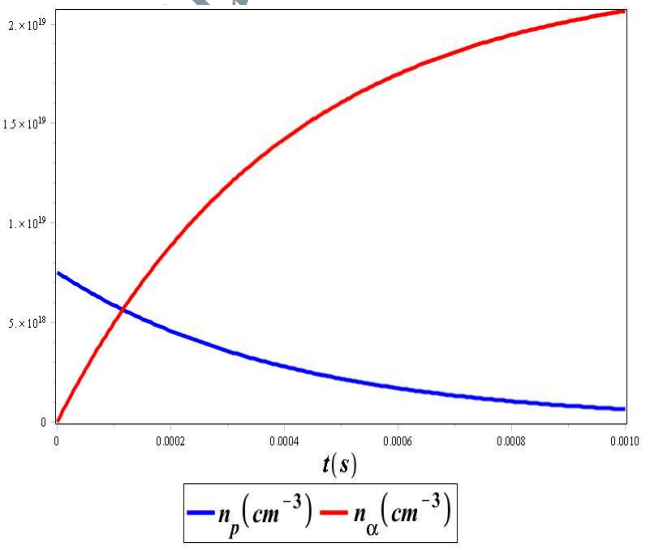

(b)

Figure 9. time variations of proton particle density, n_p, and alpha particle density,‘ n_α, in the time interval a) 0 to 5 milliseconds b) 0 to 1000 microseconds

From observing equations 21 and 22, it can be seen that the rate equations related to the density of proton and alpha particles are coupled nonlinear points. We have solved these equations according to the stated conditions and presented the results in Figure 9 in two different time intervals: a) 0 to 5 milliseconds and b) 0 to 1000 microseconds. As can be seen from this figure, in both selected time intervals, with a gradual increase in time, the proton density decreases and, conversely, the alpha particle density increases. This is because during the fusion reaction, the density of the consumed fuels decreases and the density of the products, which are the alpha particles, increases. And if the time interval increases from microseconds to milliseconds and after a certain time, these densities will reach the steady state characteristic. The density of the medium $n_0 = n_H + n_B$ is assumed to include the hydrogen density $n_H = 0.75 \cdot 10^{19}$ and the density ^{11}B, $n_B = 0.25 \cdot 10^{19}$.

5. proposed reactor

In this section, a clean and clean proton-boron 11 fusion reactor is proposed [25-27]. The performance of this reactor is not similar to that of MCF and ICF reactors. In a thermonuclear fusion reactor, the speed of particles through the SW reaches 10^9 cm/s, so that the fusion reactivity reaches its maximum value. We choose the reaction: $p + {}^{11}B \rightarrow 3\ {}^{4}He + 8.9$ MeV.The suggested reactor includes a fusion plasma with a density of mg/cm^3 related to hydrogen ions and ^{11}B. A channel of plasma or a solid fuel is irradiated by an ultra-intense laser, which produces a SW containing p-particles that enter the background plasma. The α particles caused by boron fusion collide with plasma protons and accelerate the CR. The new alphas created by the external B-fields are trapped in the mirror container.

We apply a fluid exiting our container depicted in Fig.1. The proper fluid for p ^{11}B fusion reaction is a solution $^{11}B_2H_6$with a density of 1.3 x 10^3 g/cm^3 [23]. This introduced fluid can be easily compressed and reached higher densities if necessary. To create a SW in the fusion plasma in Fig.1, we apply two PW lasers with an intensity of $10^{18}\ {}^{W}/_{cm^2}$. These lasers date back more than 30 years [18-19]. The intensity of today's lasers has increased to a maximum of $10^{22}\ {}^{W}/_{cm^2}$ at infrared wavelengths (1.6 eV). Petawatt lasers generate a semi-relativistic SW at streaming speeds. The accelerated fluid volume relate to equations 10-12 is given by:

$$V = S(\tau_L + \Delta t)u_s \approx 5.3\tau_L u_{sL} S$$

$$V = 2.5 \times 10^{-6}\left(\frac{10^{-3}\,{}^{g}/_{cm^3}}{\rho_0}\right)\left(\frac{W_L}{1kJ}\right) \qquad (23)$$

In Figure 10 we have drawn the three-dimensional variations of V in terms of ρ_0 and W_L in the range of $10^{-4} \le \rho_0 \le 1$ and $1 \le W_L \le 100$ using equation 23.

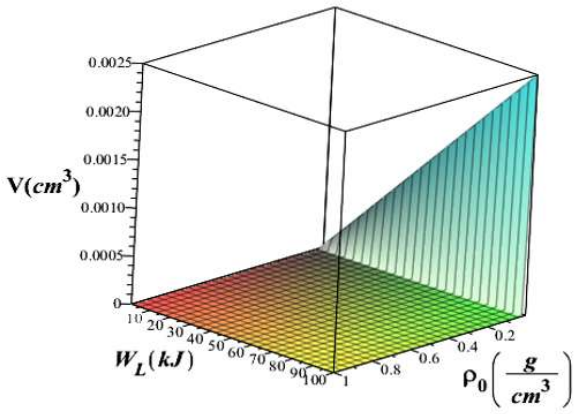

Figure 10. Three-dimensional variations of V in terms of $\rho_0$and W_L in the range of $10^{-4} \leq \rho_0 \leq 1$ and $1 \leq W_L \leq 100$

Using equations 20 to 23, we get:

$$N_{p0} = n_{p0}V = 1.25 \times 10^{14} \left\{\frac{W_L}{1kJ}\right\}$$

$$N_\alpha = 3N_{p0}\left(e^{\tau/\tau_A} - 1\right);\ \tau_A \approx 4.8 \times 10^{-5}\left(\frac{10^{-3}g/cm^3}{\rho}\right)$$

$$t \gg \tau_A : N_\alpha \approx 1.65 \times 10^{14} \left\{\frac{W_L}{1kJ}\right\} e^{\tau/\tau_A} \qquad (24)$$

In Figures 11 and 12, we have drawn the graph of N_{p0} variations in terms of W_L and the three-dimensional variations of N_α in terms of t in the range of $0.01 \leq t(ms) \leq 0.3$and $1 \leq W_L \leq 100$ using equation 24, respectively.

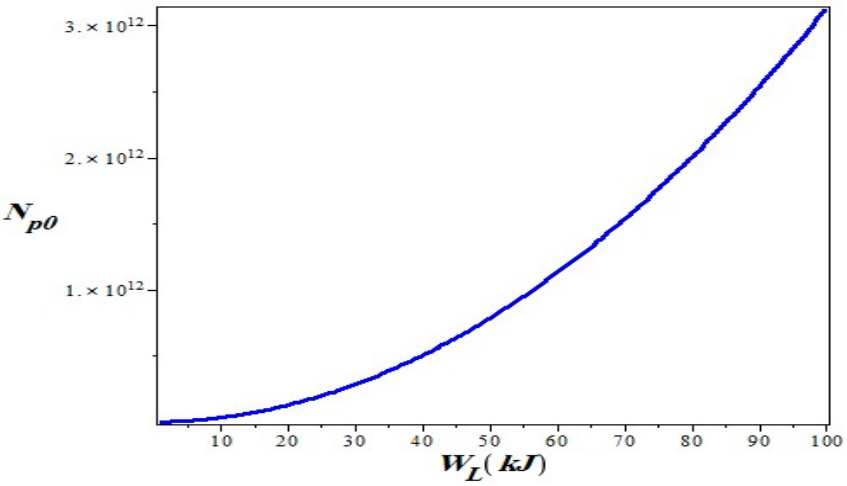

Figure 11. variations of N_{p0} in terms of W_L

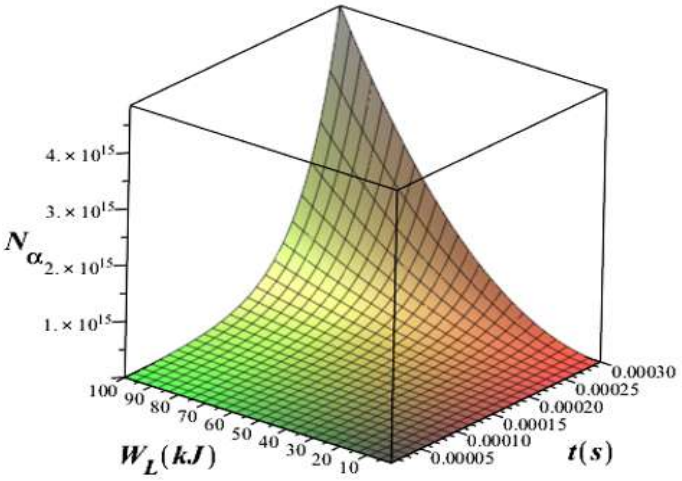

Figure 12. Three-dimensional variations of N_α in terms of t in the range of $0.01 \leq t(ms) \leq 0.3$ and $1 \leq W_L \leq 100$

We know that, the released energy from p ^{11}B fusion reaction is Q= 8.9 MeV per reaction, which is divided between 3 produced alpha particles, and let's define the fusion energy gain G in terms of $N_\alpha W_\alpha$. For laser energy W_L, $W_\alpha = {}^{8.9MeV}/_{3}$[24]. For reactor facilities, a 100 MW yield seems to be technologically and economically viable. Using equation 24, we can write:

$$G = \frac{N_\alpha W_\alpha}{W_L} = 7.8 \times 10^{-2} \exp\left(\frac{t}{\tau_A}\right) \geq 100$$

$$\exp\left(\frac{t}{\tau_A}\right) \geq 100 \rightarrow t[s] 7.15\tau_A = 3.0 \times 10^{-4} \left(\frac{{}^{10^{-3}g}/_{cm^3}}{\rho}\right) \qquad (25)$$

In Figure 13, we have drawn the variations of G in terms of time in the time range $0.01 \leq t(ms) \leq 0.3$ using equation 25. As can be seen, with the growth of time, G increased non-linearly and became it reaches more than 100.

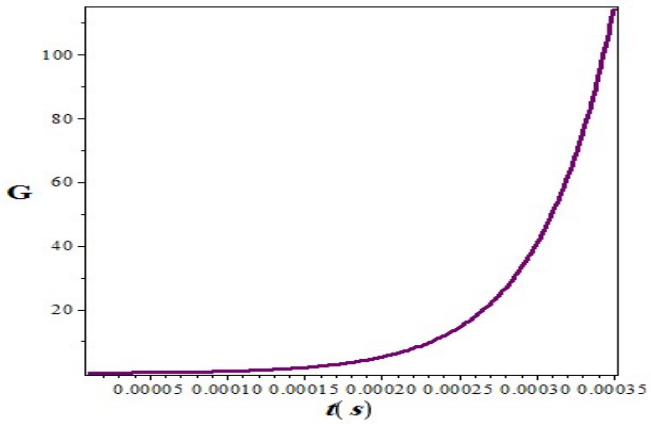

Figure 13. The variations of G in terms of time in the time range $0.01 \leq t(ms) \leq 0.3$

For each laser pulse, an external E-field with a duration of 0.3 ms is needed to obtain CR. For a 100 MW thermal fusion reactor, we need 100 laser pulses [25]. This can be done with 100 lasers at 1 Hz.

6.Conclusion

In this work, a conceptual fusion reactor was introduced by exploiting the interaction between laser and plasma and confining the fusion plasma by magnetic B-field. This reactor is made of a plasma with a density of mg.cm^{-3} containing hydrogen and boron ions. Because the temperature of this plasma is several electron volts, its radiation level is low. The mechanism of fusion starts through the channel of plasma or the solid fuel, which is irradiated by an ultra-intense laser and produces a semi-relativistic SW, which accelerates a p-beam to an energy 1200-300 keV such that the reactivity of $p^{11}B$ is sufficiently high to create 3α particles. The alphas from $p^{11}B$ collide with plasma hydrogen ions and their acceleration causes one CR, which was explained in "Containment and CRs". The thermonuclear reactor will have a maximum theoretical energy gain of 15 ~ 8900 / 600 (for the case where the alphas have the same energy). However, in the case we examined here, due to the CR mechanism, the maximum gain is (8900/600) * (CR coefficient). in which the CR coefficient is: $\exp\left[t/(n_0 < \sigma v >)\right]$ and can reach a maximum magnitude of 115. In general, in order to have a higher fusion energy gain a combination of an external E-field and a mirror magnetic confinement device should be used to induce CRs using a long laser pulse.

REFERENCES

[1] H Abu-Shawareb et al, *Phys Rev Lett* **132** 065102 (2024)

[2] A L Kritcher, A Zylstra, C Weber, O Hurricane, D A Calla-han, D S Clark, L Divol, D E Hinkel, K Humbird, O Jones et al, *Phys Rev E* **109** 025204 (2024)

[3] D S Clark, S W Haan, A W Cook, M J Edwards, B AHammel, J M Koning, and M M Marinak, *Phys Plasmas* **18** 082701 (2011)

[4] O A Hurricane, D A Callahan, D T Casey, A RChristopherson, A L Kritcher, O L Landen, S A Maclaren,R Nora, P K Patel, J Ralph, D Schlossberg, P T Springer,C V Young, and A B Zylstra, *Phys Rev Lett* **132** 065103 (2024)

[5] H Abu-Shawareb et al, **Phys Rev Lett 129** 075001 (2022)

[6] J Nuckolls, L Wood, A Thiessen, and G Zimmerman, *Nature (London)* **239** 139 (1972)

[7] J Lindl, *Phys Plasmas* **2** 3933 (1995)

[8]J Cai1, H Xie, Y Li, M Tuszewski, H Zhou and P Chen,' A study of the requirements of p-^{11}B fusion reactor by tokamak system code',Fusion Science and Technology, 78, 149-163(2022)

[9] F Debray and P Frings, "State of the art and developments of high field magnets at the "Laboratoire National des Champs Magnétiques Intenses"", Comptes Rendus Physique 14, 2 (2013) .

[10] T F Wall, "The generation of very intense magnetic fields", Electrical Engineers,Journal of the Institution of 64, 745 (1926) .

[11] B Bachmann, T Hilsabeck, J Field, N Masters, C Reed, TPardini, J R Rygg, N Alexander, L R Benedetti, T Döppner et al, *Rev Sci Instrum* **87** 11E201 (2016)

[12] A B Zylstra, A L Kritcher, O A Hurricane, D A Callahan,K Baker, T Braun, D T Casey, D Clark, K Clark, T Doppner et al, *Phys Rev Lett* **126** 025001 (2021)

[13] A L Kritcher, A B Zylstra, D A Callahan, O A Hurricane,C Weber, J Ralph, D T Casey, A Pak, K Baker, B Bachmann et al, *Phys Plasmas* **28** 072706 (2021)

[14] O A Hurricane, D A Callahan, P T Springer, M J Edwards,P Patel, K Baker, D T Casey, L Divol, T Döppner, D EHinkel et al, *Plasma Phys Control Fusion* **61** 014033 (2019)

[15] D Casey, B MacGowan, O Hurricane, O Landen, R Nora,S Haan, A Kritcher, A Zylstra, J Ralph, E Dewald et al, *Phys RevE* 108, L053203 (2023)

[16] R Hatarik et al, *J Appl Phys***118** 84502 (2015)

[17] R Betti, K Anderson, V N Goncharov, R L McCrory, DD Meyerhofer, S Skupsky, and R P J Town, *Phys Plasmas* **9** 2277 (2002)

[18] C B Yeamans and D L Bleuel, *Fusion Sci Technol* **72** 120 (2017)

[19] A B Zylstra, O A Hurricane, D A Callahan, A L Kritcher, J E Ralph, H F Robey, J S Ross, C V Young, K L Baker,D T Casey et al, *Nature (London)* **601** 542 (2022)

[20] A L Kritcher, C Young, H F Robey, C R Weber, A BZylstra, O A Hurricane, D A Callahan, J E Ralph, J S Ross,K L Baker et al, *Nat Phys* **18** 251 (2022)

[21] A L Kritcher, A B Zylstra, D A Callahan, O A Hurricane,C R Weber, D S Clark, C V Young, J E Ralph, D T Casey,A Pak et al, *Phys Rev E* **106** 025201(2022)

[22] A B Zylstra, A L Kritcher, O A Hurricane, D A Callahan,J E Ralph, D T Casey, A Pak, O L Landen, B Bachmann,K L Baker et al, *Phys Rev E* **106** 025202 (2022)

[23] M S Rubery, M D Rosen, N Aybar, O L Landen, L Divol, C V Young, C Weber, J Hammer, J D Moody, A S Moore,A L Kritcher, A B Zylstra, O Hurricane, A E Pak, SMacLaren, G Zimmerman, J Harte, and T Woods, *Phys Rev Lett* **132** 065104 (2024)

[24] O A Hurricane, D T Casey, O Landen, A L Kritcher, RNora, P K Patel, J A Gaffney, K D Humbird, J E Field,M K G Kruse et al, *Phys Plasmas* **27** 062704 (2020)

[25] J D Lindl, S W Haan, O L Landen, A R Christopherson, and R Betti, *Phys Plasmas* **25** 122704 (2018)

[26] P T Springer, O A Hurricane, J H Hammer, R Betti, D ACallahan, E M Campbell, D T Casey, C J Cerjan, D Cao,E Dewald et al, *Nucl Fusion* **59** 032009 (2019)

[27] H G Rinderknecht, D T Casey, R Hatarik, R M Bionta, B J MacGowan, P Patel, O L Landen, E P Hartouni, and O AHurricane, Phys *Rev Lett* **124** 145002 (2020)